International Journal of Architectural, Civil and Construction Sciences
ISSN: 2415-1734
Vol:13, No:9, 2019

Studying the Theoretical and Laboratory Design of a Concrete Frame and Optimizing Its Design for Impact and Earthquake Resistance

Mehrdad Azimzadeh, Seyed Mohammadreza Jabbari, Mohammadreza Hosseinzadeh Alherd

***Abstract*—**This paper includes experimental results and analytical studies about increasing resistance of single-span reinforced concreted frames against impact factor and their modeling according to optimization methods and optimizing the behavior of these frames under impact loads. During this study, about 30 designs for different frames were modeled and made using specialized software like ANSYS and Sap and their behavior were examined under variable impacts. Then suitable strategies were offered for frames in terms of concrete mixing in order to optimize frame modeling. To reduce the weight of the frames, we had to use fine-grained stones. After designing about eight types of frames for each type of frames, three samples were designed with the aim of controlling the impact strength parameters, and a good shape of the frame was created for the impact resistance, which was a solid frame with muscular legs, and as a bond away from each other as much as possible with a 3 degree gradient in the upper part of the beam.

***Keywords*—**Optimization, reinforced concrete, single-span frames, optimization methods of impact load.

I. Introduction

THE urgent need for designing and constructing structures like bridges, underground reservoirs, dams, big water reservoirs, telecommunication and energy transmission posts, silos, chimneys, marine structures, cooling towers, power stations, safe structures, harbors, etc. are the most important things to look for in today's societies. Considering certain operation conditions, some of the above-mentioned structures may be exposed to impact forces like sudden stroke of objects, sudden brake of cranes, explosion, and strokes resulting from inappropriate movement of heavy vehicles and so on. Considering that these forces are of dynamic nature (variable in time), it is important to apply suitable analytical methods to design these structures. The main objective of this paper is to offer a method to analyze stresses and displacements created in structures when they undergo impact load from different heights and the results of this study include required theoretic subjects concerning mechanics of impact on single-span concrete frames and analyzing its plasticity and offering experimental results.

Impact loading of frames was carried out according to the standard of American Association of Concrete (ACI) (this standard was defined to study the behavior of single-span frames' behavior against impact which is executed in students' competition in the said association [6]). For this purpose, an 8400 kg weight was placed inside a 4 m pipe with the diameter of 2 inches. This pipe stands on fixed legs from two sites with the height of 28 cm from the ground. There are some holes on the pipe with the diameter of 4 mm and heights of 0.5, 1.0, 1.5, 2.0, 2.5 and 3.0 m and a screw with the length of 20 cm moves easily inside them as a brace. Impact loading is started from the height of 0.5 m according to the existing standard and continues for five times from the height of 3.0 m.

Mehrdad Azimzadeh, Seyed Mohammadreza Jabbari and Mohammadreza Hosseinzadeh Alherd are with the Otaredian Company, Iran (phone: +982188374708; e-mail: Davoudbz@yahoo.com).

II. Impact Loads

An impact occurs when two or more objects hit each other. An important feature of impact is production of a relatively big force at impact point in a short time that gives a considerable momentum change to the object. Amortization is less important in control of maximum response of a structure against impact loads in comparison with dynamic periodic loads. Maximum response against an impact load comes in a very short time before amortization forces can absorb large amount of energy from the structure. The action of impact force may be internal or external. For example, a force produced from explosion of gunpowder in cannon pipe is an external force for the cannonball while it is an internal force for the wall of the cannon pipe .[3]

Analysis of dynamics of impact in structures requires information about the type of impact, impacting object and forces resulting from impact. On the whole, impact is divided into two groups, hard and soft impact. On the other hand local deformation in hard impact is small and occurs rarely in practice. Considering softness and hardness of the target and impacting object, four states were specified for the impact: [1]

- Impact of hard objects on hard targets
- Impact of hard objects on soft targets
- Impact of soft objects on hard targets
- Impact of soft objects on soft targets

Among the impacts that we experience in life, the most common type in structural affairs is the impact of hard objects on soft targets. Considering the studies carried out in this field and existing resources about soft targets, concrete and steel targets were investigated.

A. Impact on Concrete Targets

When an impact arrives at a concrete structure 5 states may occur: penetration, perforation, scabbing, spalling and punching shear (Figs. 2-5):

- Penetration (X_p): depth of pit in target in impact region

- Perforation (t_p): full penetration into the target as a result of impact with and without exitty
- Scabbing (t_{sc}): spalling of materials from back of target as a result of impact
- Spalling (t_{sp}): spalling of materials of target from impact face
- Punching Shear: separation of a piece from target on impact region

Total reaction of structure includes bending and shearing, etc. (Fig. 1)

B. Plastic Hinges in Frames

A frame under a vertical load (p) and a horizontal load (Q) is shown in Fig. 6. All parts of the frame are made of the same material and have the same intersection. If the shape of collapse of the frame is according to Fig. 6 and plastic hinges are formed in A, B, C and D, then the work of p and Q forces equals that of amortization in plastic hinges:

$$\underset{(A)}{Q.a\omega} + \underset{(C)}{p.Ac\omega\cos\theta} = \underset{(D)}{\omega M_p} + \underset{(E)}{2\omega M_p} + 2\omega M_p + \omega M_p$$

or

$$Q.a + p.b = 6M_p \qquad (1)$$

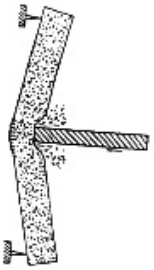

Fig. 1 Total Reaction of Target

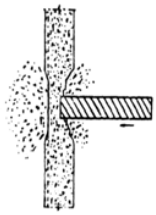

Fig. 2 Local effect of scabbing

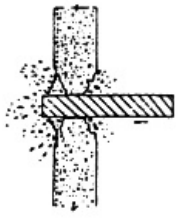

Fig. 3 Local effect of perforation

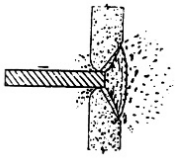

Fig. 4 Local effect of Punching shear

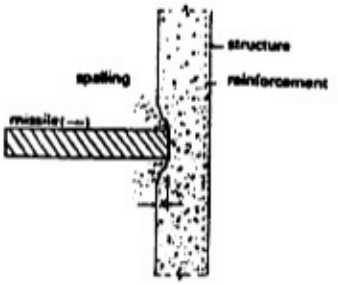

Fig. 5 Local effect of penetration

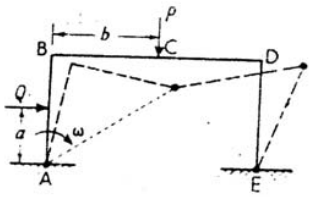

Fig. 6 A frame under a vertical load (p) and a horizontal load (Q)

We can also consider other different shapes for collapse of the frame. Finally, the state that collapses with the least load shows the real shape of collapse. [6]

III. Fixed Beam under Impact Load of a Mass

In this section, behavior of a fixed beam as 2L (Fig. 7 (a)) under an impact load of a mass (M) with initial velocity of V is being investigated.

At the time of impact, the middle of the beam moves with the velocity of V while the other parts of the beam are static. So, to create a dynamic equilibrium, suppose that the impact object is still in contact with the beam, the center-to-center distortion is supported. So, two phases of differentiated motion occur there.

In the first phase of motion, a plastic hinge is formed at t=0 and two plastic hinges are spread from the middle of the beam towards the supports (Fig. 7 (b)). In the second phase of motion, two plastic hinges at the supports and a plastic hinge in the middle of the beam are stationary (Fig. 7 (c)) and the motion of the beam and mass continues until all kinetic energy remained in mass and beam is consumed as plastic work.

First Diagram of Motion: $0 \le t \le t_1$

Index of transverse velocity on the basis of Fig. 7 (b) for right side of the beam, $0 \le x \le t_1$, can be written as:

$$\dot{w} = \dot{W}(1 - x/\xi) \qquad 0 \le x \le \xi \qquad (2a)$$

$$\dot{w} = 0 \qquad \xi \le x \le L \qquad (2b)$$

where ξ is the dependent location at the hinge.

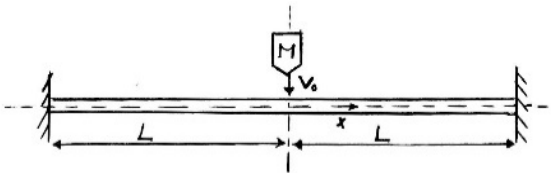

(a)

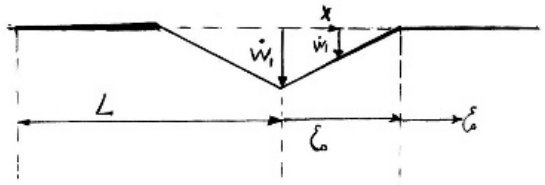

(b)

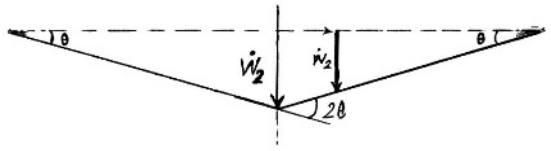

(c)

Fig. 7 (a) Stroke of mass (M) with initial velocity of V with fixed beam, (b) Index of transverse velocity for first phase of motion, $0 \le t \le t_1$, (c) Index of transverse velocity for second phase of motion $t_1 \le t \le T$

Considering that shear force Q is zero in movable hinges x= $\pm\xi$, vertical equilibrium of middle part of the beam between two movable hinges will be:

$$M\ddot{W} + 2\int_0^{\xi} m\ddot{w}dx = 0 \qquad (3)$$

By substituting (2a) into (3) we can conclude that:

$$M\ddot{W} + 2m\int_0^{\xi} [\ddot{W}(1 - x/\xi) + \dot{W}x\,\dot{\xi}/\xi^2]dx = 0 \qquad (4)$$

or

$$M\ddot{W} + m(\ddot{W}\xi + \dot{W}\dot{\xi}) = 0 \qquad (4)$$

Now, considering that $d(\dot{W}\xi)/dt = \ddot{W}\xi + \dot{W}\dot{\xi}$, integral of (4) with respect to time will be:

$$M\dot{W} + m\dot{W}\xi = MV_\circ \qquad (5)$$

Equation (5) can be written as:

$$\dot{W} = V_\circ/(1 + m\xi/M) \qquad (6)$$

Applying the equilibrium of the moment of part $0 \le x \le \xi$ with plastic hinges at x=0 and x=ξ, around the center we can conclude that:

$$2M_\circ - \int_0^{\xi} m\ddot{w}xdx = 0 \qquad (7)$$

because at X=0, M=M and at x=ξ, M= -M and Q=0, so by placing the time derivation of (2a) in (7) we will obtain:

$$\int_0^{\xi} m[\ddot{W}(1 - x/\xi) + \dot{W}\dot{\xi}x/\xi^2]xdx = 2M_\circ$$

or

$$m(\ddot{W}\xi^2/6 + \dot{W}\dot{\xi}\xi/3) = 2M_\circ$$

This equation can be written as:

$$d(\dot{W}\xi^2)/dt = 12M_\circ/m \qquad (8)$$

By integrating (8) with inspect to time and using the initial condition ζ=0 at t=0, the equation of time-distance for movable hinges will be obtained as:

$$t = m\dot{W}\xi^2/12M_\circ \qquad (9)$$

Using (6) we can write (9) as follows:

$$t = mMV_\circ\xi^2/[12M_\circ(M + m\xi)] \qquad (10)$$

By differentiating this equation with respect to time, the velocity of the movable plastic hinges will be:

$$\dot{\xi} = 12M_\circ(M + m\xi)^2/[mMV_\circ\xi(2M + m\xi)] \qquad (11)$$

From Fig. 7 (b), it is clear that transverse displacement at x, to t(x) time, when movable plastic hinge reaches at x, is zero. So, transverse displacement at x for $t \ge t(x)$ time will be:

$$w = \int_{t(x)}^{t} \dot{w}dt \qquad (12)$$

where $\dot{w}$ is shown with (2a) and t(x) time for ζ =x is calculated from (10). Equation (12) can be written as:

$$w = \int_{(x)}^{\xi} \dot{w}d\xi/\dot{\xi} \qquad (13)$$

where $\dot{\xi} = d\xi/dt$. Now by substituting (2a), (6) and (11) into (13) we will obtain:

$$w = \int_x^{\xi} \frac{V_\circ(1 - x/\xi)\,mMV_\circ\,\xi(2M + m\xi)d\xi}{(1 + m\xi/M)12M_\circ(M + m\xi)^2}$$

By integrating this equation and arranging it, W will be:

$$w = \frac{M^2 V_\circ^2}{24mM_\circ}\left\{\frac{1+\beta}{(1+\alpha)^2} - \frac{(1+2\beta)}{(1+\beta)} + \frac{2\beta}{(1+\alpha)} + 2\log_e\left(\frac{1+\alpha}{1+\beta}\right)\right\} \quad (14)$$

where;

$$\alpha = m\xi / M \quad (15a)$$

$$\beta = mx / M \quad (15b)$$

When movable plastic hinges reach at supports, the first phase of motion will be completed. So, according to (10), after substituting ζ=L, we will have:

$$t_1 = mMV_0 L^2 [12M_0 (M+mL)] \quad (16)$$

From (16), it is clear that transverse velocity is not zero at $t=t_1$. So, total kinetic energy of the mass M and beam, using (2-a) and (6) is:

$$MV_0^2 (1+2mL/3M)/[2(1+mL/M)^2] \quad (17)$$

This energy should be consumed in the second phase of the motion.

Second Phase of Motion: $t_1 \le t \le T$.

It is assumed that kinetic energy remaining at beam is consumed by two plastic hinges of supports and a central hinge at the end of first phase of motion according to (17).

Index of transverse dislocation will be as follows:

$$w_2 = (L-x)\theta \quad (18)$$

where θ is rotation angle of supports and 2θ is rotation angle of beam's center in second phase of motion. Equilibrium of energy in this phase will be as:

$$4M_0\theta = MV_0^2 (1+2mL/3M)/[2(1+mL/M)^2] \quad (19)$$

The right head side of (19) is the kinetic energy remaining at the end of the first phase, to motion (17), and its left side is the consumed energy at the plastic hinges. By substituting θ from (19) into (18), we will have:

$$4M_0\theta = MV_0^2 (1+2mL/3M)/[2(1+mL/M)^2] \quad (20)$$

Final and permanent displacement of the beam on the basis of index of Fig. 7 (a) will be obtained by summing (14), ζ=L and (20); as a result:

$$w_f = \frac{M^2 V_\circ^2}{24mM_\circ}\left\{\frac{\bar{\alpha}-\beta}{(1+\alpha)(1+\beta)} + 2\log_e\left(\frac{1+\bar{\alpha}}{1+\beta}\right)\right\} \quad 0 \le \beta \le \bar{\alpha} \quad (21)$$

where $\bar{\alpha} = mL/M$, and β is according to (15).

Special Case, Heavy Striker

In this case, at the end of first phase of motion, for ζ=L, M/mL >> 1, we can conclude from (6) that $\dot{W} \approx V_\circ$.

While assuming that M/mL >> 1, kinetic energy which should be consumed in second phase of motion, from (17) will approximately be $MV^2/2$. In other words, in this case, the first phase pf motion does not have an important role. So using the index of Fig. 7 (c), the energy equilibrium will be as follows:

$$4M_\circ \theta = MV_0^2 / 2 \quad (22)$$

In this case θ is total rotation angle of the support. Permanent transverse displacement of beam will be:

$$w_f = (L-x)\,\theta$$

or

$$w_f = MV_\circ^2 L(1-x/L)\,8M_\circ \quad (23)$$

In this case, (23) can be directly obtained from (21) considering $\beta \to 0$ and $\bar{\alpha} \to 0$.

Special Case, Light Striker

In this special case, mL/M >> 1 or M/mL → 0. As a result, at the end of first phase of motion from (6), ζ=L and $\dot{W} \approx 0$.

Kinetic energy of the mass and beam at the end of first phase of motion on the basis of (17) will be about zero. So the motion of the beam at the end of first phase of motion will be stopped when plastic hinges reach the supports.

Equation (21) can be written as:

$$w_f = \frac{M^2 V_\circ^2 L}{24M_\circ}\left\{\frac{1+\beta}{\bar{\alpha}(1+\bar{\alpha})^2} - \frac{(1+2\beta)}{\bar{\alpha}(1+\beta)} + \frac{2\beta}{\bar{\alpha}(1+\bar{\alpha})} + \frac{2}{\bar{\alpha}}2\log_e\left(\frac{1+\bar{\alpha}}{1+\beta}\right) + (3+2\bar{\alpha})(1-\beta/\bar{\alpha})(1+\bar{\alpha})^2\right\}$$

Considering that $\bar{a}$ >> 1, the following equation will be obtained:

$$w_f \approx \frac{M^2 V_\circ^2 L}{12M_\circ \bar{\alpha}} \log_e\left(\frac{\bar{\alpha}}{1+\beta}\right)$$

or

$$w_f = \frac{M^2 V_\circ^2 L}{12mM_\circ} \log_e\left(\frac{mL/M}{lmx/M}\right) \quad (24)$$

IV. Plastic-Dynamic Behavior of Beams

The trend of the expressed theory will be used to study the dynamic behavior of beams. However, the beam can be

obtained using the trend of rectangular sheet. In this section, dynamic behavior of beam will be obtained using squared yield criterion. The trend of the theory was investigated on the basis of maximum yield condition of normal tension in [2].

Dynamic Behavior of Beam with Simple Support under Temporal Dynamic Load

It is assumed that the load is spread uniformly. Analysis of rectangular sheet theory, when $\xi_\circ \to 0$ و $tg\phi = \sqrt{3}$ ، $\beta \to 0$, expresses the behavior of a beam, the length of span of which is 2B. So, total time of motion, T, is obtained as follows:

$$tg\,\gamma T = \eta\ \mathbf{sin}\ \gamma\tau/(1-\eta+\eta\mathbf{cos}\ \gamma\tau) \quad (25)$$

where

$$\gamma = (12M_\circ/\mu HB^2)^{1/2} \quad (26)$$

and the highest permanent transverse displacement will be:

$$W_f/H = \left\{[1+2\eta(\eta-1)(1-\cos\gamma\tau]^{1/2}-1\right\}/4 \quad (27)$$

Now, the following equation exists for a beam with span length of 2B:

$$\lambda\,\xi_\circ^2 = (\mu V_\circ^2 L^2/M_\circ H)(\beta tg\phi)^2 = 3\mu V_\circ^2 B^2/M_\circ H$$

So, by substituting the length of the span, 2L, for 2B, we will have $\lambda\xi_\circ^2 = 3\lambda$ while λ,

$$\lambda = \mu V_\circ^2 L^2/M_0 H \quad (28)$$

And initial kinetic energy has no dimension. So, (28) for extended steady impact velocity will be changed as below:

$$W_f/H = \left\{[1+3\lambda)^{1/2}-1\right\}/4 \quad (29)$$

It should be noted that m=μB, where m is the mass of length unit of the beam and M is the bending moment of plastic for transverse unit of the beam.

Dynamic Behavior of Beam with Fixed Supports under Temporal Dynamic Load

In this case, a trend similar to the previous one is used. So we can conclude from the equations that:

$$tg\,\gamma T = \eta\,\mathbf{sin}\,\gamma\tau/(1-\eta+\eta\mathbf{cos}\,\gamma\tau) \quad (30)$$

and

$$W_f/H = \left\{[1+\eta(\eta-2)(1-\cos\gamma\tau)/2]^{1/2}-1\ \right\}/2 \quad (31)$$

and the equation for impact load will be as follows:

$$W_f/H = [(1+3\lambda/4)^{1/2}-1\ \}/2 \quad (32)$$

V. Effect of Impact on Steel Fracture in Its Strengthening

By studying the factors of steel fracture and their formation, we can adjust the fracture of steel and its status by applying the required preparations to make it suitable to use.

Factors of steel fracture are: [4]

a) Excessive Variation of Elasticity
b) Excessive yielding or plastic deformation
c) Fracture

Fracture in metals has three types:

a) Sudden Brittle Fracture
b) Fatigue or gradual progressive fracture
c) Fracture or delay

Unlike what was assumed, soft metals also experience sudden brittle fractures under special conditions.

Under three-dimensional tension conditions, drop in temperature and increase in strain rate the fracture has more tendency to brittle fracture.

VII. Strain Rate and Its Effect on Flow Properties

Strain rate is the change of strain during the time and is shown as $\dot{\varepsilon} = d\varepsilon/dt$. Strain rate has an important effect in flow tension and increasing the strain rate will increase the tensile strength.

Yield tension and flow tension in low wax-like strains are more dependent on strain rate than tensile strength. Temperature has an important role in strain rate and is clearly sensible. Strain rate is very high in impact loadings and is of special importance. There is a considerable pre-fracture difference under impact loads and static loads. The time is not enough for diffusion of tension throughout the object in impact load, such that fracture occurs in some part of solid, without any fracture in other parts. If we consider that the speed of diffusion of fracture is about 830 m/s (6000 ft/s) and also diffusion speed of tensional waves in solids is in the range of 914 m/s to 609 m/s (3000 to 2000ft/s), we can often see that visible fracture is formed as a result of impact waves but have no time to be diffused before changing tension state. Considering what was said in this regard, it should be noted that tension waves in free surfaces and fixed selected locations are more reflected in discontinuities inside the object in places where cross-section area is changing.

Now, we want to study the structure of steel and find out how to face this type of fracture and even how to define it and increase the resistance of steel.

Steel, like other materials, is made of crystalline networks and different grains and folds.

Inside steel fractures may result from slip of grains or crystals on each other or fractures of the crystals themselves. Strengthening is also on the same basis that is desirable arrangement of crystals such that they will show a good resistance for special uses, or arrangement of grains' borders or strengthening the grains using solutions of different type. With this strengthening we can increase toughness of steel. Toughness of a material is in its capability to absorb energy in wax-like area. It is also the basic capability against tensions

higher than yield tension without fracture. Toughness is a parameter, which includes strength and softness. For example, steel with average strain has a yield and tensile structure in comparison with elastic high-carbon steel. However, the levels of strain-tension curve are higher, so it is tougher.

VIII. Making the Samples

In order to start the examinations and make the samples, impact loading jack for frames was made first. According to ACI and similar jack used in American Concrete Competitions, a pipe with the diameter of 2 inches and length of 3.5m was connected to the middle of a metal plate where a hole with the diameter of 2 inches had been made. This plate was welded to another metal plate from four sides by four legs, the length of each was 26 cm (in order to prevent energy losses resulting from loading of the frame and to transfer the energy of frame legs to base plate). Some holes with the diameter of 4 mm were created form the height of 0.5 m up to the height of 3 m such that a screw with the length of 20 cm the weight inside the tube can move easily. An 8.4 kg weight was placed into the pipe and loading jack is made ready to be used by a metal pulley.

Materials used for the manufacture of high quality concrete in mixing design:

- Cement: Cement with high Belin (about 4000), type II, produced in Soufian Cement Co.
- Micro silica: Iran Ferroalloys Industries Company
- Super plasticizer: We used common super plasticizers produced in Iran.
- Aggregate: Granite coarse aggregates, with maximum size of 4.75 cm (sieve No.4) and fine aggregates-light fine aggregates of Eskandan pumice mine. (Omran pumice Tabriz Co.)
- Air Bubble Additives: Clinic Beton Iran

TABLE I
Specifications of Concrete Mix Design

Cement's Quantity kg/m³	Micro silica kg/m³	W/ C+S.F	Water's Quantity Lit/m³	Super plasticizer kg/m³	Aggregate kg/m³		Air-entertaining Bulb kg/m³	Pressure strength (15×15)		Density of Hardened Concrete
					Coarse aggregate	Fine aggregate		7 days	28 days	
550	55	0.2	121	8.25	694	691	11	997	1391	2360

In order to decrease the weight of the frames, we had to use light fine aggregates and in case of using granite fine aggregates of about 400 kg/cm^2, the pressure strength will be increased up to 28 days. In order to reinforce the frames, according to the limitation existed in ACI for the competitions where the maximum diameter of concretes should be 1.6 mm, we used spring steel wire which had plastic stair and had more resistance against impacts in strain-tension curve and its Fy was determined as 18350 kg/cm² in steel tension test.

Relying on the theoretical literature of analyzing plastic fixed beams and single-span frames, the first frame design was made with SAP 2000, schematic picture of which is shown in Fig. 8.

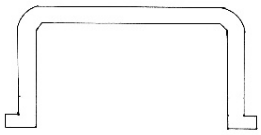

Fig. 8 Initial design of the frame

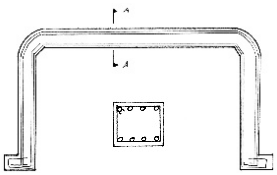

Fig. 9 Reinforcement of the original frame

Of course, the aim of this simple design was to obtain some overall conclusions and evaluate some theoretical results.

Type of reinforcing in the design is shown in Fig. 9. As it is clear, reinforcing is uniform and eight longitudinal reinforcement are seen in each cross-section and the maximum distance between two stirrups is 25 mm. Arrangement for making stirrups is the opposite of beam's tension distribution, so the stirrups will be used very optimally and will not be placed in the path of the fracture.

After that the frame of the design was made and the reinforcements were placed in the frames, mix design of concrete was prepared and put in the frame. Treatment of the frames was carried out for 28 days at 20°. After treatment, impact loading was carried out and the concrete frame tolerated a 3-meter-high impact. Then the results were analyzed and compared with theoretical results and the fracturing and place of plastic joints formed in the frame were optimized using cross-sections' optimization software. Then this cross section was designed as a rigid frame using SAP 2000 software. The schematic view is shown in Fig. 10.

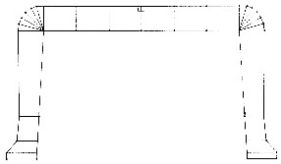

Fig. 10 Optimal design of the frame

Like the previous case, the designed frame was made and after reinforcement the mix design of concrete was prepared. Treatment was like the previous case and impact loading of the frame was carried out, the result of which was tolerating three impacts from the height of 3 m before releasing the frame. After making some other designs (each time the results

of the previous attempts were used to optimize the impact strength of the frame), it was decided to use reinforcement stairs idea. As such, two of the longitudinal reinforcement bends downward in the middle to increase the tensile strength of the frame, where the greatest tensile strength is required to withstand the impact.

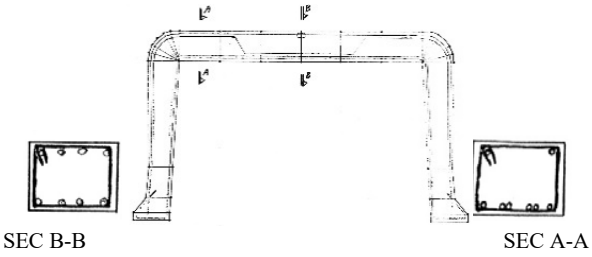

Fig. 11 Reinforcement of the optimal frame

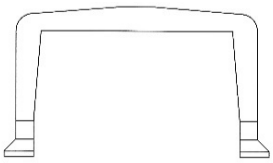

Fig. 12 Final design of the frame

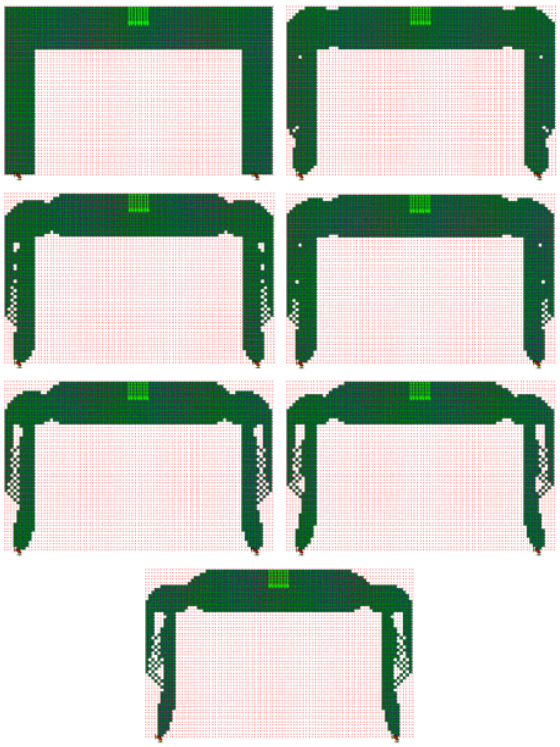

Fig. 13 Display the stages of geometric frame optimization

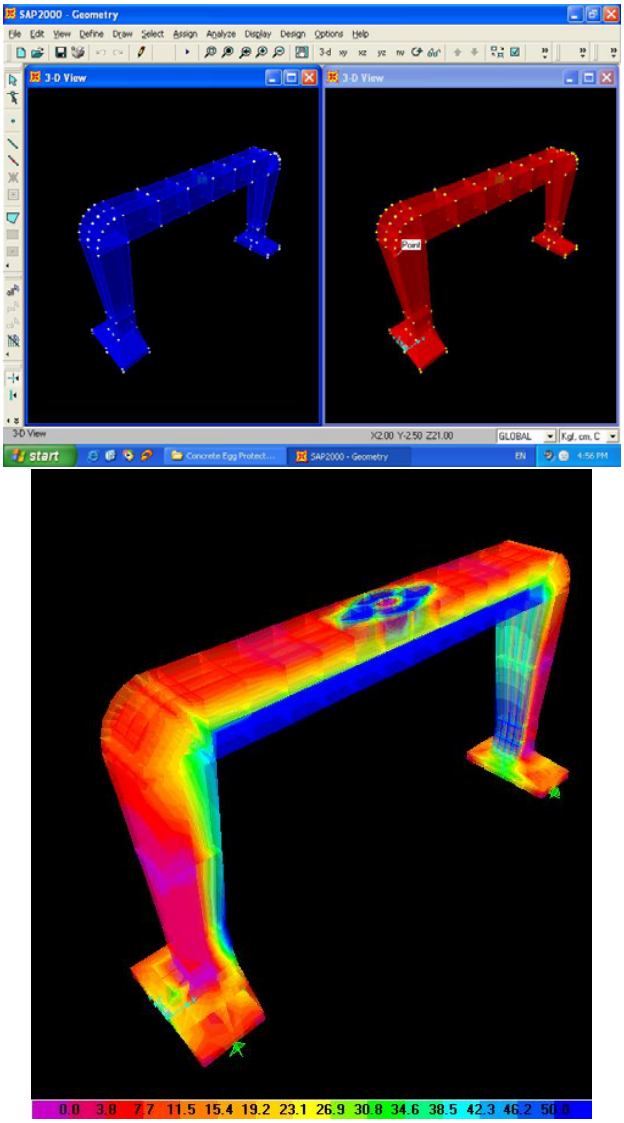

Fig. 14 Stages of optimization and frame engineering with SAP software

Up to the middle of the cross-section, the beam is bended and at that state continues its way on a straight line and then passes the middle part of the beam and bends upward and then continues its motion in its initial direction, Fig. 11. This design was made, and we obtained good results compared with previous results and this time it was decided as the armature is seen as a stair in the middle of the frame designed to increase the tensile strength. The design of these frames was designed and made but previous good results were not repeated and the results obtained here were so weak. After comparing the two recent frames with previous ones and analyzing all possible parameters, we concluded that the reason that why the design of frame with reinforcement stair provided good results was that the shape of the frame had been optimized otherwise, reinforcement stairs would have no meaning in impact loading just like static loading. After designing about eight types of

frames for each type of frames, three samples were made with the aim of controlling impact strength parameters and we obtained an optimal shape of frame for impact strength which was a completely solid frame with muscular legs and as a link away from each other, as much as possible, with the slope of 3° in the upper part of the beam. The picture is shown in Fig. 12.

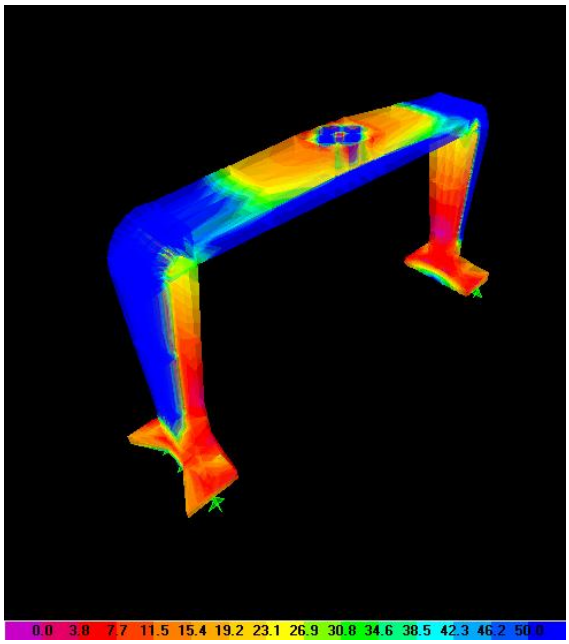

Fig. 15 Optimized frame model using SAP software

IX. Conclusion

We obtained good results with final loading of the frame such that the best result of 24 previous frames was tolerating 3 impacts from the height of 3 m but in the last frame it was 6 impacts from the height of 3 m. Although the frame was not completely released, reinforcements were leaded downward like elastic springs at the time of applying the impact after that the weight returned to its initial position. This result made us apply the results in plastic limits of spring steels and optimize them more than before. In order to do this, we decided to use Ansyse, which is complex and specialized software for simulation and modeling of the structure. As plastic analysis and modeling the frames with Ansyse in the limits of time is out of the scope of this paper, this discussion is being executed as a research project since 9 months ago and according to the schedules of the project we need one year to complete it; the final results of optimization of single-span reinforced concrete frames' resistance against impact will be offered at the end of the said project.

References

[1] Saadatpour, Mohammad Mohammadi, Dynamics of Structures, written by D.Bolio, Cliff & Joseph Penzin, Ardakan Publications, 2010.
[2] Vahedian, Ebrahim, Period of Mechanics- Vector Dynamics, Second Edition, Hosseinian technical Publications, 2013.
[3] Tahooni, Shapour, Design & Calculation of Welded Structures, Dehkhoda Publications, 2016.
[4] Dr. Mahmoud Shakeri & Dr. Abolfazl Darvizeh, Mechanics of Impact, volume 1,2, Gilan University's Publication, 2017.
[5] Cyril M. harvis and Charier E. Credem Shock and vibration handbook crede. ZD. Ed. New York, McGraw-Hill (2013).
[6] Bangosh, M.Y.H. Impact & Explosion: Blackwell Scientific Publications, London (2011).